Communication

Sensitive, Label-Free DNA Diagnostics Based on Near-Field Microwave Imaging

Barry Friedman, Mariafrancis A. Gaspar, Sergey Kalachikov, Kiejin Lee, Rastislav Levicky, Gang Shen, and Hyunjun Yoo

J. Am. Chem. Soc., **2005**, 127 (27), 9666-9667• DOI: 10.1021/ja051760i • Publication Date (Web): 16 June 2005

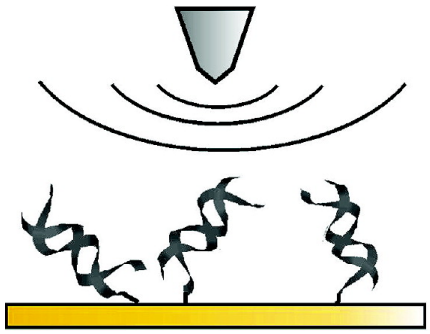

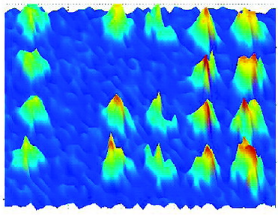

More About This Article

Additional resources and features associated with this article are available within the HTML version:

- Supporting Information
- Links to the 3 articles that cite this article, as of the time of this article download
- Access to high resolution figures
- Links to articles and content related to this article
- Copyright permission to reproduce figures and/or text from this article

View the Full Text HTML

J|A|C|S
COMMUNICATIONS

Published on Web 06/16/2005

Sensitive, Label-Free DNA Diagnostics Based on Near-Field Microwave Imaging

Barry Friedman,[†] Mariafrancis A. Gaspar,[‡] Sergey Kalachikov,[§] Kiejin Lee,*[,||] Rastislav Levicky,*[,‡] Gang Shen,[‡] and Hyunjun Yoo[||]

Department of Physics, Sam Houston State University, Huntsville, Texas 77341, Department of Chemical Engineering, Columbia University, New York, New York 10027, Columbia Genome Center, Columbia University, New York, New York 10032, and Department of Physics and Interdisciplinary Program of Integrated Biotechnology, Sogang University, Seoul 121-742, Korea

Received March 19, 2005; E-mail: RL268@columbia.edu; klee@sogang.ac.kr

Solid-phase biological diagnostics, in which biological molecules (e.g., nucleic acids, proteins) are identified through binding with complementary, immobilized biomolecules, underpin a diversity of technologies central to immuno- and DNA-diagnostics. Since the appearance of solid-phase nucleic acid assays in the 1960s based on radioisotopic detection,[1] modern assays have evolved into high-throughput microarray formats that typically rely on fluorescent labeling of the analyte. A number of alternate detection methods have been reported,[2−11] but unless some label (e.g., a fluorescent dye, a nanoparticle) is used, sensitivities remain low compared to the fluorescence "standard." Label-free diagnostics remain attractive, however, as they simplify sample preparation, decrease assay costs, and eliminate potential artifacts from label instability or perturbation of assay thermodynamics.[12] Here we demonstrate that near-field microwave imaging (NFMI) can achieve noncontact, label-free detection of low surface coverage analyte species at sensitivities comparable to conventional fluorescence bioassays.

NFMI functions by sensing changes in electrostatic coupling between a "probe" and the sample. In our design the probe is a sharpened metal wire tip in which voltage oscillations are excited at microwave frequencies.[13] Because tip−sample distances are maintained at a few tens of nm, much less than the microwave wavelength (∼ cm), tip−sample interactions occur under near-field conditions. If the sample is translated under the probe tip, changes in tip−sample coupling can be used to obtain images at resolutions (∼1 micron) below the diffraction limit.

At its other end, the probe is inserted into a microwave resonance cavity, or "resonator," populated by standing microwaves. The resonator drives the electronic oscillations in the probe. Prior to measurement, the resonator is "tuned" to equalize its impedance with that of the microwave input line (Supporting Information). Tuning consists of minimizing the voltage reflection coefficient of the resonator, $S = |Z_C - Z_I|/|Z_C + Z_I|$,[14] where Z_C is the impedance of the resonator, and Z_I, the input line impedance. Typically S of less than 10^{-3} is achieved. Since Z_C includes contributions from probe−sample interactions, tuning by necessity requires selection of a "reference state" for the sample. A change in probe−sample interactions, for example, due to binding of analyte molecules to the surface, perturbs the system from the reference state and results in an increase in S.

Figure 1a shows frequency-sweep data for S measured from a series of *n*-alkanethiol self-assembled monolayers (SAMs), at a tip−sample separation of 10 nm. Alkanethiol SAMs were used because their thickness can be systematically varied from ∼0.5 nm to over 2 nm by adjustment of the alkyl chain length. The SAMs were prepared on gold-coated glass slides, with the thickness of the gold equal to the skin depth (1.1 μm) of the microwave radiation so as to approximate a semi-infinite medium. As the frequency of the microwave source is swept, each trace in Figure 1a exhibits a minimum corresponding to the standing wave mode for that particular resonator−sample combination. The minimum is most pronounced for the butanethiol (C4) specimen, since this sample was also used as the reference state for the initial S tuning. Clear changes are evident in response to differences in SAM thickness.

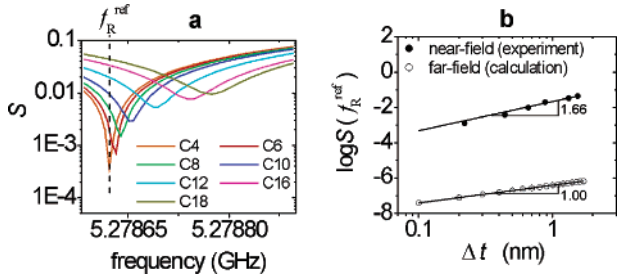

Figure 1. Near-field microwave measurements on *n*-alkylthiol ($HS-(CH_2)_{n-1}CH_3$) monolayers. Tip−sample distance: 10 nm. (a) S as a function of frequency. The butanethiol (C4) sample was used as reference for S tuning, with the minimum found at $f_R^{ref} = 5.278\ 6217$ GHz. (b) (●) log S measured under near-field conditions at 5.278 6217 GHz (dashed line in plot a), as a function of thickness increase $\Delta t = t - t_{C4}$. (○) Calculated log S for far-field reflection.

The increase in log S with film thickness, measured at the position f_R^{ref} of the C4 minimum (dashed line in Figure 1a), is plotted as the filled circles in Figure 1b. Film thickness was assumed to increase by $\Delta t = 0.22$ nm per two methylene units.[15,16] Over the investigated thickness the empirical dependence of log S on log Δt can be approximated as linear with a slope dlog S/dlog Δt of 1.66 ± 0.12, as shown in Figure 1b. This response reflects the near-field probe−sample interaction, and as such depends on probe tip geometry and the tip−sample separation. For comparison, under far-field conditions, when microwaves are incident from distances many times their wavelength on nm-thick SAM films, a weaker slope dlog$S$/dlogΔt of 1.00 is expected. Such a response is plotted in Figure 1b for 5 GHz microwaves reflecting under perpendicular incidence from a layer of lossless dielectric (i.e., a SAM) on a semi-infinite, zero-resistivity metal support, calculated following ref 17.

An important metric for future applications is sensitivity to changes in surface coverage, which requires characterization of measurement noise. Analysis of 100 independent trials (Supporting Information) revealed that, for log $S = -3.0$, which is near the tuned state when measurement is close to maximally sensitive to perturbations, the root-mean-square (rms) statistical noise in log

[†] Sam Houston State University.
[‡] Department of Chemical Engineering, Columbia University.
[§] Columbia Genome Center, Columbia University.
[||] Sogang University.

10.1021/ja051760i CCC: $30.25

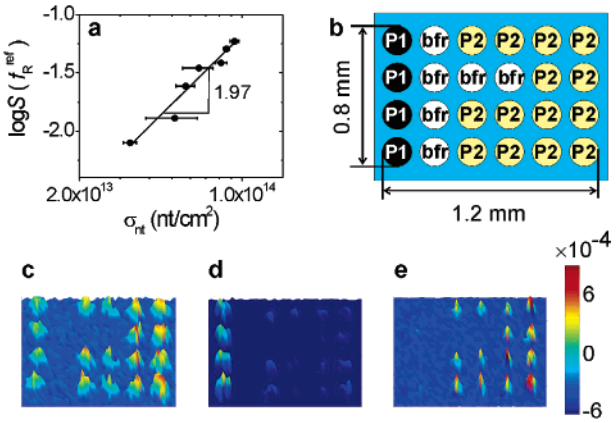

Figure 2. Near-field microwave measurements on DNA monolayers. Tip−sample distance: 10 nm. (a) Response curve for DNA monolayers, plotting log S as a function of nucleotide (nt) coverage σ_{nt}. Unmodified (DNA-free) area served as reference (f_R^{ref} = 5.271 2479 GHz). Data scatter is dominated by uncertainty in DNA coverage, not by the NFMI measurement. (b) Array layout used for hybridization imaging experiments. (c) As prepared array. The NFMI image confirms layout of immobilized P1 and P2 sequences. (d) After hybridization to sequence complementary to P1. (e) After array regeneration and hybridization to sequence complementary to P2. The hybridized images in panels d and e are difference images obtained after subtraction of the unhybridized image in panel c. The color scale spans a range in S of 7×10^{-4} for panel c and 14×10^{-4} for panels d and e.

S is 5.4×10^{-7}. From data in Figure 1b, log S of −3.0 corresponds to a Δt of 0.15 nm. Given that dlog S/dlog $\Delta t = 1.66$ it follows that an increase in thickness by 1×10^{-6} nm, from 0.15 to 0.150 001 nm, increases log S by 4.8×10^{-6}. This increase represents a signal-to-rms noise ratio (SNR) of about 9, an easily detectable change. For butanethiol with a molecular volume of 0.18 nm^3/molecule, a thickness increase of 1×10^{-6} nm corresponds to a change in coverage of discrete molecules of just 5.6×10^{12} molecules/m^2. In comparison, a full alkanethiol monolayer possesses 4.67×10^{18} molecules/m^2;[18] thus, the smallest detectable change in coverage (based on a criterion of SNR of 9) is estimated at about 1 millionths of full coverage, or about 6 molecules per square micron.

This remarkable sensitivity recommends NFMI for applications that require detection of trace surface species. As an example of such an application, films of single-stranded 21mer oligodeoxyribonucleotides (CAA TAC GCA AAC CGC CTC TCC) were prepared with different coverages on gold-coated slides following previously reported methods.[19] Nucleotide coverages were independently determined with X-ray photoelectron spectroscopy, using integrated P 2p emission from the phosphorus atoms of immobilized DNA.[20] The response curve of log$S(f_R^{ref})$ with nucleotide (nt) coverage σ_{nt}, using a DNA-free area as reference, is plotted in Figure 2a. As for the SAM films, the data can be empirically fit to a linear relationship with dlog S/dlog $\sigma_{nt} = 1.97 \pm 0.27$. For an SNR of 9, and at log $S = -2.0$ when rms noise in log S is 7.7×10^{-9} (Supporting Information), this response allows a detection of changes in σ_{nt} of 3×10^6 nt/cm^2, corresponding to 1.4×10^5 21mer strands/cm^2. This compares favorably with fluorescence-based scanners widely used in microarray applications. For example, an optimized home-built system was reported capable of detecting coverages down to 1×10^9 fluorophores/cm^2,[21] or about 300 zeptomoles (10^{-21}) in a 150 μm diameter microarray spot. The above estimates show that even if multiple fluorophores are used per strand, label-free NFMI detection can approach if not exceed the sensitivity of conventional fluorescence diagnostics.

In bioassay applications, detection is often accomplished in an array format. For investigating this type of sample a prototype array was prepared consisting of two immobilized sequences, P1 (CAA TAC GCA AAC CGC CTC TCC) and P2 (CGT TGT AAA ACG ACG GCC AG) (Figure 2b). Buffer (bfr) spots were also printed as a control. NFMI images were scanned at a 25 micron resolution in x and y. Figures 2c−e show S images of the as-prepared array (Figure 2c) and after hybridization to sequences complementary to the P1 (Figure 2d) or the P2 (Figure 2e) spots. The hybridized data are displayed as difference images in which the unhybridized image was subtracted. Sequence-specific hybridization is the dominant change identified.

The principal advantage of NFMI over other label-free detection methods is outstanding sensitivity, thus removing a central obstacle to label-free diagnostics. As with other label-free approaches, however, a significant disadvantage is susceptibility to nonspecific background. In the absence of a label to enhance contrast between species of interest and other material, such as water or salt residue, a label-free technique requires stricter control over sample preparation and measurement. We anticipate that this remaining challenge can be partially resolved by in situ measurements under a buffer environment.

Acknowledgment. Support for this work was provided by the National Science Foundation (DMR-00-93758; DMR-02-13574; BES-04-28544; DMR-03-07170), by the Korea Research Foundation (KRF-2002-015-CS0018; KRF-2002-005-CS0003), and by Sogang University (20031503).

Supporting Information Available: Description of experimental procedures and data for S noise analysis. This material is available free of charge via the Internet at http://pubs.acs.org.

References

(1) Gillespie, D.; Spiegelman, S. *J. Mol. Biol.* **1965**, *12*, 829−842.
(2) Palecek, E.; Fojta, M.; Tomschik, M.; Wang, J. *Biosens. Bioelectron.* **1998**, *13*, 621−628.
(3) Taton, T. A.; Mirkin, C. A.; Letsinger, R. L. *Science* **2000**, *289*, 1757−1760.
(4) Janshoff, A.; Galla, H.-J.; Steinem, C. *Angew. Chem., Int. Ed.* **2000**, *39*, 4004−4032.
(5) Fritz, J.; Baller, M. K.; Lang, H. P.; Rothuizen, H.; Vettiger, P.; Meyer, E.; Guntherodt, H.-J.; Gerber, C.; Gimzewski, J. K. *Science* **2000**, *288*, 316−318.
(6) Isola, N. R.; Stokes, D. L.; Vo-Dinh, T. *Anal. Chem.* **1998**, *70*, 1352−1356.
(7) Cao, Y. C.; Jin, R.; Mirkin, C. A. *Science* **2002**, *297*, 1536−1540.
(8) Lin, V. S.-Y.; Motesharei, K.; Dancil, K.-P. S.; Sailor, M. J.; Ghadiri, M. R. *Science* **1997**, *278*, 840−843.
(9) Lu, J. H.; Strohsahl, C. M.; Miller, B. L.; Rothberg, L. J. *Anal. Chem.* **2004**, *76*, 4416−4420.
(10) Brockman, J. M.; Nelson, B. P.; Corn, R. M. *Annu. Rev. Phys. Chem.* **2000**, *51*, 41−63.
(11) Piunno, P. A. E.; Krull, U. J.; Hudson, R. H. E.; Damha, M. J.; Cohen, H. *Anal. Chem.* **1995**, *67*, 2635−2643.
(12) Naef, F.; Magnasco, M. O. *Phys. Rev. E* **2003**, *68*, 011906.
(13) Kim, J.; Lee, K.; Friedman, B.; Cha, D. *Appl. Phys. Lett.* **2003**, *83*, 1032−1034.
(14) Pozar, D. M. *Microwave Engineering*; Addison-Wesley: New York, 1990; p 77.
(15) Porter, M. D.; Bright, T. B.; Allara, D. L.; Chidsey, C. E. D. *J. Am. Chem. Soc.* **1987**, *109*, 3559−3568.
(16) Bain, C. D.; Whitesides, G. M. *J. Phys. Chem.* **1989**, *93*, 1670−1673.
(17) Silva, E.; Lanucara, M.; Marcon, R. *Supercond. Sci. Technol.* **1996**, *9*, 934−941.
(18) Strong, L.; Whitesides, G. M. *Langmuir* **1988**, *4*, 546−558.
(19) Johnson, P. A.; Levicky, R. *Langmuir* **2003**, *19*, 10288−10294.
(20) Shen, G.; Anand, M. F. G.; Levicky, R. *Nucleic Acids Res.* **2004**, *32*, 5973−5980.
(21) Cheung, V. G.; Morley, M.; Aguilar, F.; Massimi, A.; Kucherlapati, R.; Childs, G. *Nat. Genet.* **1999**, *21*, 15−19.

JA051760I